BIOCHEMISTRY
including biophysical chemistry & molecular biology

Article

pubs.acs.org/biochemistry

Multiple Exosites Distributed across the Three Domains of Streptokinase Co-Operate to Generate High Catalytic Rates in the Streptokinase−Plasmin Activator Complex

Rachna Aneja, Manish Datt, Suman Yadav, and Girish Sahni*

The Institute of Microbial Technology (CSIR), Sector 39-A, Chandigarh-160036, India

Supporting Information

ABSTRACT: To examine the global function of the key surface-exposed loops of streptokinase, bearing substrate-specific exosites, namely, the 88−97 loop in the α domain, the 170 loop in the β domain, and the coiled-coil region (Leu^{321}-Asn^{338}) in the γ domain, mutagenic as well as peptide inhibition studies were carried out. Peptides corresponded to the primary structure of an exosite, either individual or stoichiometric mixtures of various disulfide-constrained synthetic peptide(s) inhibited plasminogen activation by streptokinase. Remarkably, pronounced inhibition of substrate plasminogen activation by the preformed streptokinase−plasmin activator complex was observed when complementary mixtures of different peptides were used compared to the same overall concentrations of individual peptides, suggesting co-operative interactions between the exosites. This observation was confirmed with streptokinase variants mutated at one, two, or three sites simultaneously. The single/double/triple exosite mutants of streptokinase showed a nonadditive, synergistic decline in k_{cat} for substrate plasminogen activation in the order single > double > triple exosite mutant. Under the same conditions, zymogen activation by the various mutants remained essentially native- like in terms of nonproteolytic activation of partner plasminogen. Multisite mutants also retain affinity to form 1:1 stoichiometric activator complexes with plasmin when probed through sensitive equilibrium fluorescence studies. Thus, the present results strongly support a model of streptokinase action, wherein catalysis by the streptokinase−plasmin complex operates through a distributed network of substrate-interacting exosites resident across all three domains of the cofactor protein.

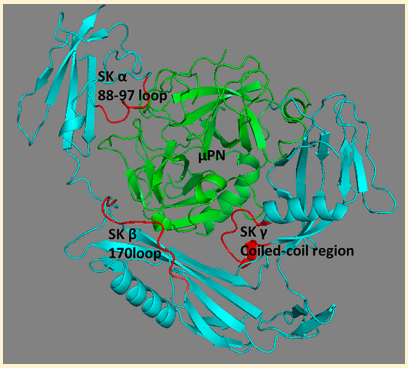

Streptokinase (SK), a bacterial thrombolytic protein, acts by forming an equimolar stoichiometric complex with human plasmin(ogen) (HPG), leading to the activation of substrate HPG to form plasmin (HPN), which then dissolves the fibrin clots. HPG, upon its complexation with SK, undergoes a conformational alteration and forms an amidolytically active (SK·HPG*) complex, which activates substrate HPG through selective proteolytic scission of the scissile Arg561-Val562 peptide bond in HPG to form HPN (via the so-called Pathway I, also referred to as the conformational activation pathway; see Figure 1).[1−4] Alternatively, SK can either directly complex with free HPN, or the SK·HPG* activator complex can preferentially exchange with free HPN, to form the fully mature SK·HPN activator complex indirectly since HPN possesses three orders of higher affinity for SK compared to that for HPG (Pathway II; direct proteolytic pathway; Figure 1).[5,6] Free plasmin essentially possesses a broad trypsin-like substrate preference (along with a low affinity to bind with lysine residues of fibrin due to the kringle domains). However, as stated above, plasmin, upon complexation with the cofactor SK, develops a unique, high degree of substrate specificity directed predominantly toward the scissile peptide bond in HPG.[7]

Streptokinase is an enzymatically inert bacterial cofactor. Structurally, it consists of three conformationally homologous domains (α, β, and γ), which are separated by two highly flexible linkers, and small flexible regions at the amino and carboxy termini.[4,8] Various binding studies suggest that SK

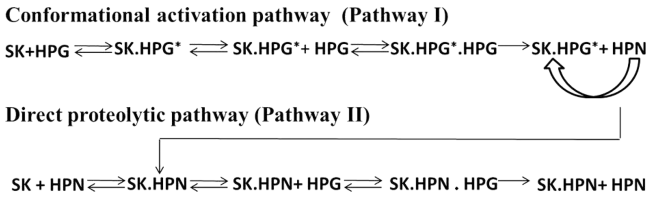

Figure 1. Schematic representation of the steps involved in the activation of HPG by SK. SK forms an equimolar complex with HPG (Pathway I) that leads to the generation of an active center in the complex (SK·HPG*) without cleavage of the scissile peptide bond in the partner HPG. This virgin complex then recruits free HPG as the substrate and converts it to HPN. The HPN so formed rapidly exchanges the HPG* from SK·HPG* complex due to its multifold higher affinity for SK in comparison to that for HPG. Alternatively, the SK can directly combine with the HPN to make the SK·HPN activator complex (Pathway II). The activator complex then catalytically acts on substrate HPG molecules and converts them into HPN.

Received: February 4, 2013
Revised: August 6, 2013
Published: August 6, 2013

   dx.doi.org/10.1021/bi400142s | *Biochemistry* 2013, 52, 8957−8968

induces the expression of substrate recognition exosites/epitopes on the SK·HPG activator complex, which transforms HPN from an indiscriminate Lys/Arg residue-specific serine proteinase to a highly substrate-specific proteinase.[9−12] In addition, HPG activation rates by the SK·plasmin(ogen) activator complex are recognized to be highest among all known plasminogen activators.[13] This inordinately high catalytic turnover by the SK·plasmin(ogen) activator complex can also be attributed to its three-domain architecture, elucidated through previous domain truncation studies.[14,15] These studies suggest that the interdomain co-operativity among the three linked domains of SK results in long-range protein−protein interactions between the SK·HPG activator complex and its multidomain substrate, HPG. These interactions are perhaps the underpinnings for the generation of both strong enzyme−substrate affinity and turnover (catalytic) rates of HPG activation. Domain truncation studies from our laboratory, in the past, suggest that different bidomain derivatives of SK, such as $\alpha\beta$ and $\beta\gamma$, are fairly capable of docking the macromolecular substrate nearly as efficiently as the native, tridomain SK molecule, but the catalytic rates generated by the former are extremely low.[14] There is thus a lacuna in quantitative corelation between the docking ability of the substrate and subsequent catalytic turnover. This prompts us to conclude that the three-dimensional docking of substrate is only an important determinant in the initial narrowing of the specificity of the SK·HPG active center and enzyme−substrate complex stabilization.[4] The catalytic spark generated at the active site upon the docking of macromolecular substrate needs to be amplified further in terms of the high turnover numbers associated with the fully functional SK·HPG activator complex. However, the exact interdomain interactions responsible for this process, e.g., those between the three domains of SK with partner HPN and those of the activator complex with substrate HPG, and, finally, ones responsible for postdocking and/or postcleavage steps such as product expulsion, are little understood at present.

Obtaining fundamental insights into the mechanism underlying the design principles of SK·HPG activator complex, wherein a protein cofactor redirects the specificity and rate of a catalytic process by long-range interactions, is important in the general understanding of this therapeutically important system. A rough guide to the structural topology of SK gauged through peptide walking, especially with regards to HPG binding,[9,16] followed by high resolution X-ray diffraction studies,[4,17] suggests that SK consists of various structural motifs, such as small, surface-exposed loops, distributed across its three domains, that can potentially interact with an incoming substrate molecule. Subsequently, a series of site-specific mutagenesis-based studies have successfully identified some of the important loops/epitopes involved in enzyme−substrate interactions. For example, an epitope in the α domain, namely, the 88−97 loop, plays an important catalytic role through its interaction with the serine protease domain of substrate HPG,[11] whereas in the β domain, the 170 loop has been recently identified as a catalytically important exosite.[12] Remarkably, none of these sites have been shown to confer any substantial enzyme−substrate affinity, but (as their mutations show) these are nevertheless important in generating high catalytic rates for plasminogen activation by the SK·HPG complex. In contrast, the 250 loop in the β domain had earlier been shown to selectively enhance the affinity of the SK·HPG activator complex with substrate HPG through kringle mediated interactions.[18,19] Also, charged residues in the so-called coiled-coil region of the gamma domain are known to be involved in substrate HPG activation;[20,21] however, the exact mechanism whereby this region is important catalytically in substrate catalysis (namely, enhancing substrate turnover without conferring substrate affinity per se) has been elucidated only recently.[21] Even though the above-mentioned studies do provide an identity to the sites whereby substrate HPG interacts with the SK·HPG complex, whether the sites act independently or in concert remains an important mechanistic question demanding a resolution.

In the current study, an attempt toward this has been made through relatively simple approaches, namely, peptide inhibition, on the one hand, and by multiple-exosite mutagenesis experiments on the other. Interestingly, the results presented below, on individual single-, double-, and triple-site mutants of SK altered in the 88−97 and 170 loops and the coiled-coil region, reveal that there indeed exists a remarkable cooperativity among the various SK exosites in processing substrate HPG. Thus, for the first time, the present investigation unveils a global function to the various exosites of SK by demonstrating their concerted action during substrate HPG activation.

EXPERIMENTAL PROCEDURES

Reagents. Glu-plasminogen was either purchased from Roche Diagnostics Inc. or purified from human plasma by affinity chromatography.[22] The T7 RNA polymerase-promoter-based expression vector, pET 23(d), and *Escherichia coli* strain BL21 (DE3) were products of Novagen Inc. (Madison, WI). Thermostable DNA polymerase (*pfu Turbo*) was obtained from Stratagene Inc. (La Jolla, CA). Custom-oligonucleotide primers were supplied by Biobasic, Inc., Canada. Phenyl agarose 6XL was procured from Prometic Biosciences Ltd., Isle of Man, U.K., and DEAE-aepharose (fast-flow) from Pharmacia Amersham-GE, Uppsala, Sweden. Urokinase, EACA, sodium cyanoborohydride, and L-lysine were purchased from Sigma Chemical Co., St. Louis, MO. All other reagents used were of the highest analytical grade available.

Peptide Synthesis. Custom synthesis of the peptides, namely, the 88−97 loop, Glu^{86} to Val^{100} (CQLIANVHSNDDYFEVC), 170 loop, Pro^{165} to Leu^{185} (CQFTPLNPDDDFRPGLKDTKLLC), coiled-coil region, Leu^{321} to Asn^{338} (CLDFRDLYDPRDKAKLLYNC), and control peptide, Val^{20} to Ser^{34} (CVSVAGTVQGTNQDISC) derived from the primary structure of SK was carried out using standard Fmoc, (*N*-(9-fluorenyl)-methoxycarbonyl)-based Merrifield solid-phase peptide chemistry on an automated peptide synthesizer model-PS3 by M/s USV, Mumbai, India. After synthesis and cleavage by standard procedures, the peptides were purified on RP-HPLC in a standard acetonitrile−0.1% trifluoroacetic acid system, and the disulfide constrained peptides were oxidatively cyclized by H_2O_2 treatment. The thiol groups, as measured by Ellman's reagent (DTNB) were found to be oxidized by this treatment; mass spectra (MALDI/ESI) of the peptides also confirmed that the peptides were oxidized as indicated by a reduction of mass by approximately 2 Da (MALDI/ESI data shown in Figure S1, Supporting Information). The secondary structures of the three peptides were also determined through Far-UV CD spectroscopy. Peptides were dissolved in water at 0.5−1.0 mg/mL concentration, and their CD spectra were recorded on a JASCO 810 instrument, using a cuvette with a path length of 0.1 cm. The secondary structure was determined using JASCO software.

Design and Construction of Various SK Multisite Loop Mutants. The SK gene from *Streptococcus equisimilis* H46A strain, a type C *Streptococcus*, was earlier cloned in a pET-23d vector,[23] and this construct was used to prepare all substitution mutants. The various substitution mutants of the three domains of SK were prepared using the QuickChange Mutagenesis kit obtained from Stratagene Inc., which involves the usage of two complementary primers having the desired mutation at the center.

Expression and Purification of *wt*SK/SK Multisite Loop Mutants. The *wt*SK and the various exosite mutants cloned in pET23d were expressed intracellularly in *E. coli* BL21(DE3) cells as inclusion bodies (IBs) under the control of the T7 phage RNA polymerase promoter after induction with isopropyl-1-thio-β-D-galactopyranoside (IPTG), solubilized, and purified as described.[23]

Preparation of HPN. Plasmin (HPN), the active form of HPG, was prepared by digesting Glu-HPG with UK (urokinase) covalently immobilized on agarose beads using a ratio of 300 Plough units/mg HPG in 50 mM Tris·Cl, pH 8.0, 25% glycerol, and 25 mM L-lysine at 22 °C for 10 h.[23]

Preparation of Active-Site Fluorescent Labeled HPN. N^{α}-[(acetylthio) acetyl]-D-Phe-Pro-Arg-CH_2Cl (ATA-FPR-CK) was prepared by mixing 5 mg of D-Phe-Pro-Arg-CH_2Cl (FPR-CK), (procured from Bachem) in 50 mM sodium phosphate buffer, pH 7.0, with 0.5−1 volume of succinimidyl (acetylthio)acetate (SATA, Molecular probes) in methanol to give a final concentration of 3−6 mM FPR-CK and a 4−5-fold molar excess of SATA.[24,25] After incubating the reaction mix for 30 min at room temperature, the reaction was stopped with Tris·Cl at pH 8.0 to get ATA-FPR-CK. The active site of HPN was then specifically inhibited by the above-obtained ATA-FPR-CK in sodium phosphate buffer at pH 7.0, and its inhibition was measured by the residual activity of the chromogenic substrate, H-D-Val-Leu-Lys-*p*-nitroanilide·2HCl (S-2251). After the complete inhibition of HPN, it was labeled with 5-(iodoacetamido) fluorescein (5-IAF), and fluorescein incorporation was determined to be in the range of 0.9−1.0 mol of fluorescein/mol of HPN, as described.[10]

Assays for Determining the Inhibition of the HPG Activator Activity of the Preformed *wt*SK·HPG Complex by Peptides Comprising Amino Acid Sequence(s) of Various Exosites of SK, i.e., the 88−97 Loop, 170 Loop, and the Coiled-Coil Region in the γ Domain. The SK·HPG activator complexes were formed by preincubating equimolar concentrations (0.5 μM each) of SK and HPN in 50 mM Tris·Cl, pH 7.5, and 0.5% BSA at 25 °C for 1 min.[26] This enzyme complex was added to reaction mixes to obtain a final concentration of 5 nM, already containing various equimolar combinations of individual peptides, at a final concentration of 900 μM overall, in assay buffer containing 50 mM Tris·Cl at pH 7.5 and 100 mM NaCl preincubated with 0.05 μM HPG for 10 min. The generation of plasminogen activator activity was measured spectro-photometrically at 405 nm by recording the increase in rate of release of *p*-nitroanilide from the chromogenic substrate, Chromozym-PL (tosyl-Gly-L-Pro-L-Lys-pNA) by the human plasmin generated as a result of HPG activation for a period of 10 min at 25 °C. Control reactions contained all components except the test peptide. The specific activity at each combination of inhibitory peptides was calculated by obtaining the slopes of the activation progress curves as change in absorbance/t^2.[9,16] The extent of inhibition by different concentrations of a given peptide was determined and expressed as a percentage relative to control reactions (taken as 100%) conducted in the absence of peptide.

Assays for Studying the Activation of HPG by *wt*SK and SK Mutants. A one-stage colorimetric assay method was used to measure the kinetics of HPG activation by *wt*SK or its mutants.[27,28] The change in absorbance at 405 nm was then measured as a function of time (t) in a Molecular Devices Versamax microplate reader at 25 °C. The activator activities were obtained from the slopes of the activation progress curves as change in absorbance/t^2 [27,28] using a linear fit equation of the Origin 7.0 version of the software.

N-Terminal Methionine Removal from *wt*SK/SK Multisite Loop Mutants. The N-terminal methionine was removed from *wt*SK and various mutants using methionine amino-peptidase (*pfu* MetAP) enzyme by a procedure described earlier.[29] The extent of removal of the N-terminal methionine was determined by N-terminal sequence analysis on a Applied Biosystems protein sequencer, Model 491A, and also through quantitative amino acid composition analysis using a Waters Pico-Tag system.

Esterolytic Activation of Equimolar HPG·SK/SK Multisite Loop Mutant Complexes. To monitor the active site formation in the SK·HPG complex, 7 μM HPG was added to an assay cuvette containing 7.5 μM *wt*SK/mutant, 100 μM NPGB, and 10 mM sodium phosphate buffer at pH 7.5. The burst of *p*-nitrophenol released due to acylation of the active center was monitored at 410 nm as a function of time at 25 °C.[1,30,31]

Determination of the Steady-State Kinetic Constants for the Amidolytic Activity of SK/SK Multisite Mutants. SK/SK multisite mutants and HPN were precomplexed at 4 °C in equimolar ratios (100 nM each) for 1 min in 50 mM Tris·Cl at pH 7.5 containing 0.5% BSA. The amidolytic activity was measured by transferring an aliquot of this mixture to a 100 μL reaction well of a 96-well plate containing buffer (50 mM Tris·Cl) and varying concentrations of the chromogenic substrates, namely, Chromozym-PL (tosyl-Gly-L-Pro-L-Lys-pNA) (0.1−2.0 mM) and S-2444 (L-PyroGlu-Gly-L-Arg-pNA) (0.5−5.0 mM) to obtain a final concentration of 10 nM of the complex in the reaction. The reaction was monitored spectrophotometrically at 405 nm for 5 min at 25 °C. The kinetic constants were calculated by standard methods.[30]

Fluorescence Binding Studies. Fluorescence measurements were made with a Cary Eclipse fluorescence spectrophotometer using acrylic cuvettes coated with polyethylene glycol-20,000. Fluorescence titrations were measured at the excitation and emission wavelength maxima for the 5-IAF labeled HPN at 513 and 525 nm, respectively. Fluorescence titrations were performed as described,[10] and the fluorescence measurements were expressed as the fractional change in the initial fluorescence $(F_{obs} - F_o)/F_o = \Delta F/F_o$. The titrations were analyzed by nonlinear least-squares fitting of the quadratic binding equation with maximum fluorescence change ($\Delta F_{max}/F_o$), dissociation constant (K_D), and stoichiometric factor (n) as the fitted parameters as described.[10]

Determination of Steady-State Kinetic Constants for HPG Activator Activity of *wt*SK/SK Multisite Loop Mutants. The kinetics of HPG activation by *wt*SK/SK loop mutant·HPN complexes were measured by transferring suitable aliquots (so as to attain 0.5 nM final conc in the assay mix) of preformed *wt*SK/SK loop mutant·HPN complexes to the reaction wells containing varying concentrations of substrate HPG (0.1 μM−2 μM) in assay buffer (50 mM Tris·Cl buffer at

dx.doi.org/10.1021/bi400142s | *Biochemistry* 2013, 52, 8957−8968

pH 7.5 and 100 mM NaCl) also containing 0.5 mM chromogenic substrate Chromozym-PL. The generation of activator activity was monitored at 25 °C at 405 nm, as before. The kinetic parameters for HPG activation were then calculated from Michaelis–Menten (V versus S) and inverse ($1/V$ versus $1/S$) Lineweaver–Burk plots.[26]

Kinetic Analysis of Protein–Protein Interactions by Surface Plasmon Resonance-Based Ternary Interaction Analysis. A surface plasmon resonance-based biosensor was also used to measure the rate and equilibrium dissociation constants describing interactions between soluble analytes HPG and *wt*SK/SK multisite mutants complexed with immobilized HPN, a situation simulating substrate binding to the binary complex and hereafter referred to as a ternary interaction, as described previously.[18] Experiments were performed at 25 °C in HBS running buffer (30 mM Hepes, pH 7.4, 135 mM NaCl, and 1 mM EDTA) supplemented with 0.05% Tween 20 and 5 mM NPGB. The NPGB was included in order to prevent plasmin-mediated proteolysis.[18] After subtracting the nonspecific response, the association rate constants (k_{on} values), the dissociation rate constants (k_{off} values), and the equilibrium binding constants (K_D) were calculated from sensorgrams by nonlinear fitting of the association and dissociation curves according to a 1:1 binding model, using BIACORE 3000 evaluation software.

Molecular Modeling and Docking Studies for the Generation of μPN·SK·μPN$_{substrate}$ Ternary Complex. Cartesian coordinates of the SK β domain, SK·μPN complex, and staphylokinase (SAK) ternary complex, namely, the μPN·SAK·μPN complex, were retrieved from the Protein Data Bank (PDB IDs 1C4P, 1BML, and 1BUI, respectively).[4,17,32] Coordinates for the 170 loop and 250 loop in the β domain of SK are missing in the SK·μPN crystal structure due to the high flexibility of the two disordered loops.[4] However, coordinates for these two loops are intact in the isolated β domain crystal structure (PDB ID 1C4P).[17] The coordinates for the β domain in the SK were replaced with those of the isolated β domain, and the structure was energy-minimized for a total of 2000 steps with a combination of steepest descent and conjugant gradient algorithms without any cut off for the calculation of nonbonded interactions in implicit solvent using the FF03 force-field. Subsequently, rigid body docking of the energy-minimized structure of SK onto the μPN$_{(substrate)}$·μPN$_{(partner)}$ complex derived from the ternary complex coordinates of SAK·μPN$_{(partner)}$·μPN$_{(substrate)}$[32] was performed using ZDOCK.[33] A total of 100 docked conformations were generated. SAK, being structurally homologous to the SK α domain,[4] is known to share the same target sites on the HPG surface.[34,35] On the basis of the structural equivalency of the SK α domain in the SK·μPN complex with that of the SAK in the ternary complex of SAK·μPN $_{(partner)}$·μPN $_{(substrate)}$, scoring of the modeled complex was done. Rescoring of docked conformations was then performed based on their root-mean-square distance (RMSD) with respect to the structure of the SK·μPN complex.[4] This step ensured that the relative orientation of SK and cofactor μPN was the same as that observed in the crystal structure,[4] with the substrate μPN optimally positioned in the active site valley of the SK·μPN complex. Docked conformation with minimum RMSD was taken for further investigation.

RESULTS

Inhibition of the Activator Activity of the Preformed *wt*SK·HPG Enzyme Complex by Peptides Corresponding to the Primary Structures of the Various Exosites of SK. To investigate the possible existence of co-operativity among various exosites of SK during the activation of HPG, a set of cyclic peptides constrained through incorporation of an intramolecular disulfide bond (see Experimental Procedures for details) were custom-synthesized. These synthetic peptides encompassed the primary structures of the various exosites of SK known to date,[36] namely, residues Glu^{86} to Val^{100} for the 88–97 loop,[11] residues Pro^{165} to Leu^{185} for the 170 loop,[12] and residues Leu^{321} to Asn^{338} of the SK gamma domain. The circular dichorism analysis of the three peptides suggested that although they tend to adopt disordered structure in solution, they also showed 20–30% turn-like structures, which are concordant with their original structures predicted through X-ray diffraction data on SK·μPN and isolated β domain (PDB IDs 1BML and 1C4P, respectively) using the DSSP program[37,38] (data are shown in Table S1 in Supporting Information). We then examined these peptides for their ability to inhibit HPG activation by the preformed *wt*SK·HPG enzyme complex. The peptides were taken individually and also in their various combinations (see also, refs 9 and 16 for earlier work with SK using a peptide walking approach). The extent of inhibition in the initial rates of SK·HPG-mediated substrate HPG activation by the different cyclic peptides compared to uninhibited controls is shown in (Figure 2). Interestingly, the corresponding linear peptides and a control cyclic peptide corresponding to residues Val^{20} to Ser^{34} of the N-terminal region of SK did not show any observable inhibition in a similar concentration range (see Figure 2). The inhibitory effect for all three exosite peptides followed a dose–response inhibition up till 300 μM concentration, but the extent of inhibition by all of the individual exosite peptides did not increase beyond 30–50% inhibition at a concentration of approximately 300 μM and above (see Figure S2, Supporting Information). Interestingly, much more inhibition in HPG activation was observed when peptides encompassing residues of the above-mentioned exosites were used in combinatorial cocktails as compared to their single-exosite peptide reactions, conducted with each peptide alone with the same overall final concentration (see Figure 2 showing inhibition at one of the representative concentrations of the peptides and Experimental Procedures for other details). For example, at 900 μM final concentration, each of the peptides encompassing the 88–97 loop, 170 loop, and coiled-coil region exhibited ~50% inhibition toward HPG activation. When, at the same effective overall concentration as above, equimolar mixtures of two different peptides, namely, the 88–97 loop +170 loop, the 88–97 loop + coiled-coil region, or the 170 loop + coiled-coil region combinations, were studied for inhibiting HPG activation, the results revealed much higher inhibition in HPG activation (~75–80%) in all three cases. The reaction in which all three peptides were mixed in equimolar concentrations to achieve the same overall (900 μM) effective concentration, a less than 10% activation of HPG (i.e., more than 90% inhibition), was observed, clearly indicating a nonadditive effect in thwarting HPG activation. Another notable point is that relatively high concentrations (900 μM) of the peptides were required to attain the observed inhibitions in the catalytic rates of plasminogen activation by SK·HPG (used at 5 nM in the assays) at substrate HPG conc of

dx.doi.org/10.1021/bi400142s | *Biochemistry* 2013, 52, 8957–8968

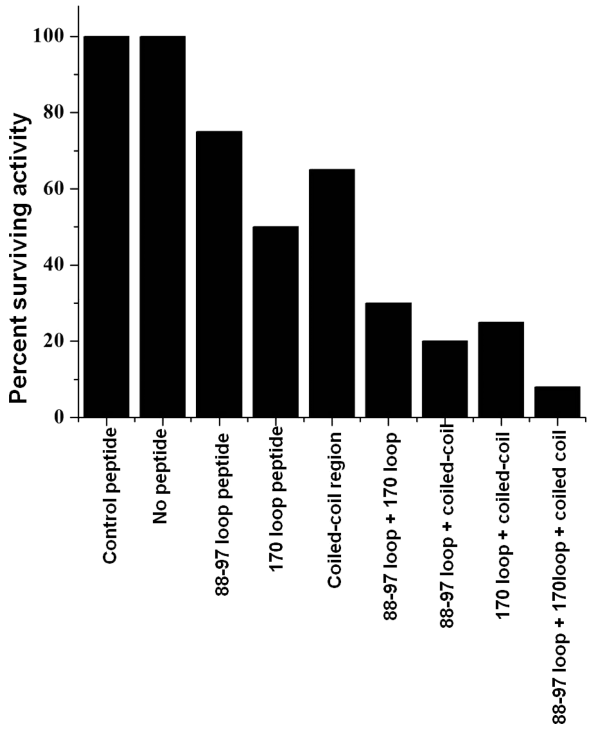

Figure 2. Representative data showing the inhibition of substrate HPG activation with the *wt*SK·HPN activator complex, employing individual control peptides, exosite-based peptides, or with exosite peptide mixtures. Synthetic peptides carrying the sequence of the three exosites in SK, namely, the 88−97 loop of the alpha domain, 170 loop of the beta domain, and the coiled-coil region of the gamma domain were analyzed as described in the text. Aliquots of preformed SK·HPN complex (5 nM) were added to HPG (0.05 μM) in assay buffer containing equal concentrations of various disulfide-constrained synthetic peptides, either individually or in different combinations of the three exosite-corresponding peptides, i.e., either two-peptide combinations or a three-peptide combination (final conc of 900 μM in all cases). Residual percent activity in the presence of different individual exosite peptides or in their various combinations is presented as bar graphs, calculated from the rates of plasmin generated in the presence of peptides compared with that of the activation reaction (taken as 100%) where no peptide was added (see Experimental Procedures for details).

approximately 0.05 μM, which clearly testifies to the notion that these exosites do not contribute substantially to enzyme−substrate affinity per se (it likely being generated from other interactions) even though these must necessarily serve as contact points during catalysis for the competitive inhibition to take place, albeit at high concentrations of the peptides.

Simultaneous Mutagenesis at the Exosites in Streptokinase and Functional Characterization of the Multisite Mutants. The apparent synergy observed in inhibition of substrate HPG activation by the *wt*SK·HPG complex in the presence of peptides prompted us to examine whether these exosites also exhibited any co-operative interaction during the enzyme's interaction with substrate HPG. Previous studies[11,12,21] had identified discrete residues whose mutation in the above exosites resulted in significant attenuation in the catalytic rates for substrate HPG activation by the SK·HPG enzyme complex. For this, we selected representative mutants that were earlier shown to be functionally altered, e.g., a SK mutant ($SK_{88-97\text{-}BetaTurn}$) in the 88−97 loop wherein two closely spaced β-turns were introduced within this loop through four simultaneous single-residue substitutions. (Residues in *wt*SK namely Ile-88 and Val-89, altered to Pro and Ala, respectively, and residues Asp-95 and Asp-96, altered to Ser and Lys, respectively.) The resultant mutant exhibits a catalytic efficiency that was just one-fourth as compared to *wt*SK.[11] Similarly, a single substitution mutant, namely, K180A of the 170 loop, which had shown a nearly 10-fold drop in catalytic activity[12] with no alteration in substrate HPG affinity, was also selected. Likewise, mutants in the coiled-coil region of SK, namely, D328G, K3334E, and G344D, which have been earlier shown to have functional relevance in HPG activation selectively at the level of catalytic turnover of substrate,[20,21,39] were also chosen for further study.

Different double- and triple-exosite mutants were prepared carrying simultaneous mutations in the three exosites, and the respective proteins were purified to near-homogeneity (see Experimental Procedures for details). The structural integrity of different proteins was established through Far-UV CD spectroscopy and proteolysis experiments (data not shown). The CD spectra of various exosite mutants were found to be closely similar to that of *wt*SK, which, in turn, was in concordance with the spectrum reported in literature,[40] suggesting the absence of any major structural destabilization as a result of the multiple mutagenesis in SK.

The various multisite mutants of SK were then characterized with respect to their HPG activation ability as monitored through single-stage continuous spectrophotometric assays.[41] The results (shown in Figure 3) reveal the progress curves of

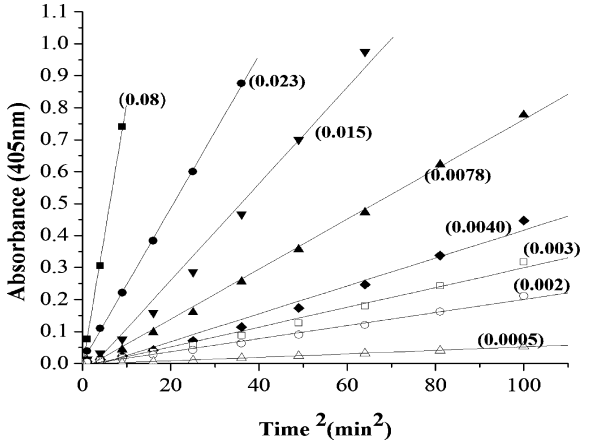

Figure 3. Time-course of single-stage HPG activation assays by *wt*SK and various exosite SK mutants. SK/various mutants of SK (0.5 nM each) were added individually to microtiter plate wells containing HPG and Chromozym-PL, and the activator activities were measured spectro-photometrically at 405 nm as detailed under Experimental Procedures. The panel shows wild type SK (■), (SK88-97-BetaTurn) (●), K180A (▲), K334E (▼), (SK88-97-BetaTurn) + K180A (○), (SK88-97 BetaTurn) + K334E (♦), K180A + K334E (□), (SK88-97-BetaTurn) + K180A + K334E (△). (Slopes of the fitted lines are shown in parentheses.)

plasmin generation as a function of the square of time by various single-, double-, and triple-site mutants of SK. The relative slopes of the progress curves exhibit considerably higher decline in HPG activator activity in the case of the double- and triple-site mutants as compared to their single-site counterparts. Double mutants comprising the above-mentioned single-site mutants in different combinations, like ($SK_{88-97\text{-}BetaTurn}$) + K180A, ($SK_{88-97\text{-}BetaTurn}$) + D328G,

dx.doi.org/10.1021/bi400142s | *Biochemistry* 2013, 52, 8957−8968

K180A + D328G, K180A + K334E, exhibited 25−30 -fold reduction in their HPG activator activity. Triple-site mutants carrying all of the above-mentioned mutants in three exosites, such as ($SK_{88-97\text{-BetaTurn}}$) + K180A + K334E, exhibited further decline viz. nearly 100-fold decline in activity compared to that of *wt*SK. The overall results suggest that decline in HPG activator activity follows a hierarchical trend, i.e., as the level of mutation increases in SK (from single site to double and further to triple site), a progressively steeper decline in HPG activator activity is notable. From the above results, the presence of cooperativity among various exosites of SK is discernible, which is in concordance with the indications obtained from the peptide inhibition experiments.

Interaction of the Various Multisite Mutants of SK with Partner HPG and HPN. Since multisite mutagenesis in SK resulted in significant reduction of HPG activator capability, it was of interest to critically examine whether the fall in substrate activation rates was due to any alteration in amidolytic/zymogen activation ability or truly because of an impaired catalytic turnover of the SK·HPG activator complex against the macromolecular substrate, HPG. Zymogen/amidolytic activation assay of HPG, the rate-limiting step in HPG activation, was performed for the different SK mutants as described in Experimental Procedures. Since the presence of the native N-terminal residue (isoleucine) in SK is required for zymogen/esterolytic activation,[42−44] all of the mutants of SK were subjected to MetAP treatment (see Experimental Procedures), and the mutants were then mixed with equimolar concentrations of HPG and examined for their ability to induce an active site in the HPG moiety of the activator complex. The results (Figure 4) clearly suggest that the single-, double- and multiexosite mutations in SK did not alter SK's ability to induce the formation of a NPGB-reactive active site since all of the double- and triple-site mutants gave a characteristic native-like NPGB burst as seen in the case of *wt* and single-site-mutated SK. Thus, these results constitute an important functional test

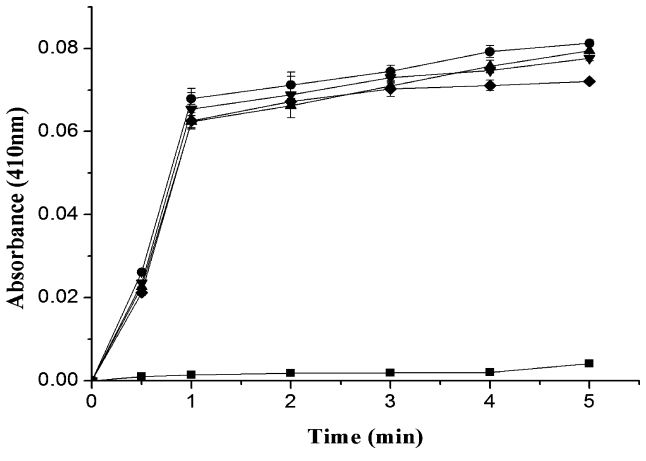

Figure 4. Active-site titration of HPG on complexing with *wt*SK/SK multisite mutants using the active-site acylating agent NPGB. The figure shows progress curves of NPGB hydrolysis as followed by color generation because of *p*-nitrophenol liberation by MetAP treated *wt*SK (●) and MetAP treated (SK88-97-BetaTurn) (▲), MetAP treated (SK88-97-BetaTurn) + K180A (▼), and MetAP treated (SK88-97-BetaTurn) + K180A + K334E (♦) complexes with HPG, and a control reaction (■) where no activator was taken (see Experimental Procedures for details).

for the native-like survival of Pathway I capability in the catalytically compromised mutants.

An alternate mechanism to zymogen activation after 1:1 complexation between SK and HPG is when SK directly binds with HPN to form a high affinity activator complex,[43,45] thus initiating the activation of substrate HPG via Pathway II.[10] Equilibrium binding studies with active-site-labeled fluorescent HPN derivatives suggest that formation of a stable high-affinity SK·HPG complex is important for its interaction with substrate HPG.[10,44,46] Therefore, during the present study, it was important to exclude the possible dissociation of mutant SK·HPN complexes under the conditions of activator assays. Accordingly, the various multisite SK mutants were examined for their capability to form high- affinity complexes with HPN by sensitive fluorescence-based procedures reported earlier.[10,44,46]

Analysis of the titrations of SK/SK multisite mutants with fluorescein-labeled HPN (Figure 5) indicates that various

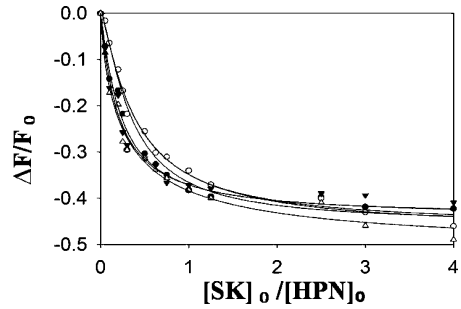

Figure 5. Fluorescence titrations of 5-(iodoacetamido) fluorescein labeled HPN with wild type SK and exosite mutants of SK to determine affinities of their 1:1 interactions. The fractional change in fluorescence ($\Delta F/F_o$) is plotted versus the ratio of varied concentrations of SK/exosite mutant with labeled HPN, prepared by inactivation with ATA-FPR-CH_2Cl and labeling with the thiol-reactive probe, 5-(iodoacetamido) fluorescein. The lines represent the least-squares fits of the binding equation for the fluorescence titrations performed and analyzed as described under Experimental Procedures. The fitted curves of change in fluorescence as a function of the ratio of [SK]/[HPN] concentrations of *wt*SK (○), (SK88-97-BetaTurn) (●), (SK88-97-BetaTurn) + K180A (△), (SK88-−97-BetaTurn) + K180A + K334E (▼).

single-, double-, and triple-site mutants bind with high affinity with HPN as does *wt*SK. The dissociation constants obtained for the various SK multisite mutants were indistinguishable from that of *wt*SK, which is in the range of 10 ± 2 pM (Table 1). The average stoichiometric factor determined from the titrations of the exosite mutants was estimated to be 1.1 ± 0.6 mol of SK/SK mutant per mol of labeled HPN. Overall, these results strongly indicate that Pathway II is native-like in even the multisite mutants. From the above study, it becomes evident that the multiple mutagenesis in SK that resulted in their significantly lowered HPG activator activity was a genuine decline and did not owe its origin to an altered affinity for HPN during the formation of the mature SK·HPG activator complex.

Steady-State Kinetics for the Amidolytic Activation by SK/SK Multisite Mutants. In order to obtain the functional characteristics of the active site, the kinetic constants associated with the processing of small molecular weight (MW) amidolytic peptide substrates, namely tosyl-glycl-prolyl-lysine-4-nitranilide acetate (Chromozym-PL; see Experimental Procedures) and L-pyroglu-glycl-arginine-4-nitranilide acetate

Table 1. Fluorescence Titration Parameters for *wt*SK and SK Exosite Mutants with 5-IAF Active Site Labeled HPN[a]

SK/SK mutants	maximum fluorescence change F_{max}/F_o	equilibrium dissociation constant K_D ($\times 10^{-12}$) M	stoichiometric factor n (mol of SK/mol of HPN)
*wt*SK	−42 ± 1%	10 ± 1	1.1 ± 0.2
($SK_{88-97\text{-BetaTurn}}$)	−50 ± 2%	12 ± 2	1.2 ± 0.1
K180A	−43 ± 2%	11 ± 1	1.1 ± 0.1
K334E	−45 ± 1%	11 ± 1	1.3 ± 0.1
($SK_{88-97\text{-BetaTurn}}$) + K180A	−48 ± 1%	12 ± 1	1.2 ± 0.3
($SK_{88-97\text{-BetaTurn}}$) + K334E	−47 ± 3%	13 ± 1	1.3 ± 0.2
K180A + K334E	−44 ± 2%	14 ± 2	1.1 ± 0.3
($SK_{88-97\text{-BetaTurn}}$) + K180A + K334E	−48 ± 2%	13 ± 1	1.2 ± 0.2

[a]The fluorescence titrations were performed by sequential additions of SK/SK mutants to labeled HPN, as described under Experimental Procedures and analyzed by nonlinear least squares fittings of the quadratic binding equation to determine the following parameters. The data represent the mean of three independent determinations.

(S-2444) were measured by the equimolar complexes of HPN with SK or the various SK multisite mutants. The results (Table 2) suggest that k_{cat} values exhibited either by SK·HPN or by SK multisite mutants·HPN complexes for the small MW peptide substrates were essentially similar to that of free HPN. However, the K_m values of the SK·HPN complex as well as different SK multisite mutants complexed with HPN for low-MW amidolytic substrates were roughly 3−4-fold higher compared to those of free HPN (see Table 2). It should be mentioned that the binding of *wt*SK to HPN results in a roughly 5-fold increase in K_m for the amidolytic substrate without a concomitant alteration in the k_{cat} values,[47] which has been attributed to a decreased accessibility of the small substrates for the active center in the HPN moiety of the activator complex, probably due to steric hindrance arising from SK binding in the vicinity of the active site.[31] The results obtained suggest that the basic characteristics of the HPN active site in terms of catalytic processing of specific peptides upon complexing with *wt*SK and different multisite mutants remain unaltered.

Steady-State Kinetics of Plasminogen Activation by Equimolar Complexes of the Various Multisite Mutants with Plasmin Shows Synergistic Decline in Their Catalytic Turnover, with No Significant Alterations in Enzyme−Substrate Affinity. To characterize the substrate HPG processing ability of different SK mutants, steady-state kinetic parameters of the multisite mutants were determined. SK/SK mutant·HPN enzyme complexes were allowed to selectively activate substrate HPG under controlled conditions, and the plasmin formed was measured spectrophotometrically.[45,48] The results (Table 3) revealed that the apparent affinity for substrate HPG is, at most, minimally altered for the various single, double, and triple mutants of the three different exosites as indicated by their K_m values (K_m ~0.5 μM in case of *wt*SK) but that they exhibited significantly reduced k_{cat} values for HPG activation when compared to those of *wt*SK. The steady state kinetic constants also show that, as reported previously, the representative mutant of the 88−97 loop (namely, $SK_{88-97\text{-BetaTurn}}$) had its catalytic efficiency reduced nearly 4-fold as compared to that of *wt*SK,[11] the SK K180A mutant of the 170 loop had catalytic turnover that was about 10% of *wt*SK,[12] and various single-site mutants of the coiled-coil region, namely, D328G, SK334E, and G344D exhibited around 10-fold decline in k_{cat} compared to that of *wt*SK.[21] When these single-site mutants were combined to form seven different double mutants, as listed in Table 3, their kinetic parameters indicated a clear nonadditive/synergistic fall in catalytic activity, nearly 25−30-fold, compared to that of *wt*SK. Since the mutant ($SK_{88-97\text{-BetaTurn}}$) exhibits slightly reduced affinity for substrate HPG, as indicated by its higher K_m value, all its double mutants, such as ($SK_{88-97\text{-BetaTurn}}$) + K180A, ($SK_{88-97\text{-BetaTurn}}$) + D328G, or ($SK_{88-97\text{-BetaTurn}}$) + K334E, also exhibited K_m values similar to that of one of their K_m-altered parent, namely, $SK_{88-97\text{-BetaTurn}}$. This suggests that apparent substrate binding ability can be independent of the concerted decline in catalytic turnover observed in the case of the double mutants. All of the triple-site mutants, namely, ($SK_{88-97\text{-BetaTurn}}$) + K180A + D328G and ($SK_{88-97\text{-BetaTurn}}$) + K180A + K334E, and ($SK_{88-97\text{-BetaTurn}}$) + K180A + G344D showed a further sharp decrease in catalytic efficiency, which was merely a 0.5% or 200-fold drop, compared to that of *wt*SK. Interestingly, in

Table 2. Steady-State Kinetic Parameters for the Amidase Activity of Equimolar Complexes of SK or the Various Exosite Mutants and HPN, and Free HPN[a]

activator species	chromozym-PL K_m (mM)	chromozym-PL k_{cat} (min^{-1})	chromozym-PL k_{cat}/K_m (min^{-1}/mM)	S-2444 K_m (mM)	S-2444 k_{cat} (min^{-1})	S-2444 k_{cat}/K_m (min^{-1}/mM)
free HPN	0.2 ± 0.06	32 ± 2	160	1.0 ± 0.1	8.0 ± 0.4	8.0
*wt*SK	0.5 ± 0.01	32 ± 2	160	3.1 ± 0.2	6.0 ± 0.4	1.9
($SK_{88-97\text{-BetaTurn}}$)	0.6 ± 0.02	34 ± 2	56	3.4 ± 0.3	6.7 ± 0.1	1.9
K180A	0.7 ± 0.04	35 ± 1	50	4.0 ± 0.3	6.0 ± 0.1	1.5
K334E	0.6 ± 0.04	33 ± 1	55	2.8 ± 0.2	6.0 ± 0.3	2.1
($SK_{88-97\text{-BetaTurn}}$) + K180A	0.8 ± 0.04	36 ± 2	45	4.2 ± 0.4	5.5 ± 0.3	1.3
($SK_{88-97\text{-BetaTurn}}$) + K334E	0.7 ± 0.05	32 ± 1	45	4.8 ± 0.2	5.0 ± 0.3	1.0
K180A + K334E	0.6 ± 0.03	36 ± 2	60	3.0 ± 0.2	4.8 ± 0.4	1.6
($SK_{88-97\text{-BetaTurn}}$) + K180A + K334E	0.7 ± 0.04	37 ± 2	52	4.6 ± 0.2	5.0 ± 0.3	1.0

[a]For the determination of the amidolytic parameters *wt*SK/SK multi-site mutants were pre-complexed with HPN in an equimolar ratio, and an aliquot of this mixture was assayed for amidolysis at varying concentrations of two chromogenic substrates with different peptide sequences, namely, chromozym-PL (Tos-Gly-L-Pro-L-Lys-pNA) and S-2444 (L-PyroGlu-Gly-L-Arg-pNA) as described under Experimental Procedures. The data represent the mean of three independent determinations.

dx.doi.org/10.1021/bi400142s | *Biochemistry* 2013, 52, 8957−8968

Table 3. Steady-State Kinetic Parameters for HPG Activation by Equimolar Complexes of SK or the Various Exosite Mutants and HPN[a]

activator species	K_m (μM)	k_{cat} (min^{-1})	k_{cat}/K_m ($min^{-1}\mu M^{-1}$)	factor (n)
*wt*SK	0.40 ± 0.05	7.5 ± 0.3	19.00	1
($SK_{88-97\text{-BetaTurn}}$)	0.9 ± 0.01	2.3 ± 0.2	2.0	3
K180A	0.5 ± 0.01	0.7 ± 0.1	1.40	10
D328G	0.6 ± 0.02	0.6 ± 0.1	1.0	12
K334E	0.7 ± 0.01	1.0 ± 0.2	1.4	7
G344D	0.5 ± 0.03	1.0 ± 0.2	2.0	7
($SK_{88-97\text{-BetaTurn}}$) + K180A	1.0 ± 0.3	0.1 ± 0.1	0.1	75
($SK_{88-97\text{-BetaTurn}}$) + D328G	1.1 ± 0.3	0.15 ± 0.01	0.136	50
($SK_{88-97\text{-BetaTurn}}$) + K334E	1.2 ± 0.3	0.2 ± 0.01	0.16	38
($SK_{88-97\text{-BetaTurn}}$) + G344D	0.9 ± 0.3	0.2 ± 0.01	0.2	38
K180A + D328G	0.6 ± 0.2	0.08 ± 0.01	0.1	83
K180A + K334E	0.7 ± 0.2	0.09 ± 0.02	0.12	83
K180A + G344D	0.6 ± 0.1	0.08 ± 0.02	0.13	100
($SK_{88-97\text{-BetaTurn}}$) + K180A + D328G	1.2 ± 0.1	0.02 ± 0.01	0.016	500
($SK_{88-97\text{-BetaTurn}}$) + K180A + K334E	1.3 ± 0.1	0.04 ± 0.01	0.03	200
($SK_{88-97\text{-BetaTurn}}$) + K180A + G344D	1.1 ± 0.2	0.03 ± 0.01	0.027	250

[a]The kinetic parameters for substrate HPG activation were determined at 25 °C with the chromogenic substrate, namely, chromozym-PL (Tos-Gly-L-Pro-L-Lys-pNA) in 50 mM Tris·Cl buffer, pH 7.5, 100 mM NaCl, as described under Experimental Procedures. The factor (n) depicts the decrease in k_{cat} compared to that of *wt*SK. The data represent the mean of three independent determinations.

spite of their extremely low catalytic activity, these multiple-site mutants still exhibited substrate affinity comparable to that of *wt*SK, except in the case of all ($SK_{88-97\text{-BetaTurn}}$) containing bi- and trisite mutants where the 2−3-fold decrease in substrate affinity exhibited by the ($SK_{88-97\text{-BetaTurn}}$) mutant continued to be retained (but not further amplified). Thus, it is safe to conclude that the various exosite mutants of SK are not significantly altered in apparent substrate affinity, in sharp contrast to the progressive manner (as the mutational load increases) in which they are compromised in terms of their catalytic rates. This observation, along with the peptide inhibition data, strongly suggests that substrate HPG processing to product HPN occurs through a co-operative interaction of the three exosites spread across the tridomain architecture of SK.

Real-Time Surface Plasmon Resonance Studies for Ternary-Mode Interactions of Various Exosite Mutants with Substrate HPG. In order to directly validate the conclusions of steady-state kinetic studies, real-time binding parameters of ternary interactions between HPG and SK/SK multisite mutants complexed to immobilized biotinylated-HPN were determined employing the surface plasmon resonance (SPR) technique. The data (Table 4), which are broadly consistent with the steady-state kinetics results, show that equilibrium dissociation constants (K_D) of ternary interaction between HPG and various single (~0.2 μM), double (~0.4 μM), and triple (~0.4 μM) exosite mutants of SK were, at

Table 4. Association (k_{on}) and Dissociation (k_{off}) Rate Constants and Apparent Equilibrium Dissociation (K_D) Constants for the Interaction of Substrate Plasminogen with *wt*SK/SK Exosite Mutants Complexed with Immobilized HPN by Surface Plasmon Resonance (SPR)[a]

	ligate HPG		
ligand	k_{on} (M^{-1} s^{-1}) ($\times 10^5$)	k_{off} (s^{-1}) ($\times 10^{-1}$)	K_D (M) ($\times 10^{-6}$)
*wt*SK	12 ± 1.5	1.8 ± 0.2	0.15 ± 0.03
($SK_{88-97\text{-BetaTurn}}$)	8.0 ± 1.0	3.5 ± 0.1	0.43 ± 0.05
K180A	11 ± 2.0	1.5 ± 0.3	0.14 ± 0.02
K334E	13 ± 2.0	1.6 ± 0.2	0.12 ± 0.01
($SK_{88-97\text{-BetaTurn}}$) + K180A	8.0 ± 1.0	3.3 ± 0.1	0.41 ± 0.03
($SK_{88-97\text{-BetaTurn}}$) + K334E	7.0 ± 1.0	3.0 ± 0.3	0.42 ± 0.01
K180A + K334E	10 ± 2.0	1.3 ± 0.3	0.13 ± 0.02
($SK_{88-97\text{-BetaTurn}}$) + K180A + K334E	9.0 ± 1.8	4.0 ± 0.2	0.44 ± 0.04

[a]The steady-state kinetic constants for the interaction of substrate HPG with *wt*SK/exosite mutants/HPN (binary complex/es) were determined by global fitting to a 1:1 binding model, using the BIAcore 3000 evaluation software as described under Experimental Procedures. A stable binary complex between *wt*SK/SK loop mutants and HPN immobilized on to the SA chip was first made, and the binding of varying concentrations of substrate HPG (0.05-1μM) was monitored.

most, minimally different compared to that for *wt*SK (~0.1 μM). It is worth noting that as compared to the docking of HPG on to the binary complex of SK, the ($SK_{88-97\text{-BetaTurn}}$) mutant and its double and triple mutant counterparts dock substrate HPG with an affinity that is 2-fold lower in magnitude. It is clearly evident from the present results that multiple exosite mutations in SK, although resulting in sharply reduced catalytic efficiency, have virtually no effects on substrate binding other than that directly contributed by one of the sites. These direct binding results are in concordance with the steady-state kinetic results, and both of these together, firmly establish that the three different exosites in SK, namely, the 88−97 and 170 loops, and the coiled-coil region, do not significantly impart enzyme−substrate affinity.

Molecular Modeling and Docking Studies Suggest Selective Interaction of Exosites in SK with the Catalytic Domain of Substrate Plasminogen. In order to obtain a molecular-level rationalization for the observed co-operativity, a ternary model of SK·μPN enzyme complexed with docked substrate (μPG) (see Figure 6) was obtained as described in Experimental Procedures. From the modeling approach, it becomes evident that the cofactor SK confers large exosite surfaces to the enzyme complex onto which the substrate can dock in the correct orientation. This is probably a vital prerequirement for re-focusing the nonspecific nature of the active center to a highly targeted specificity for the scissile peptide bond of HPG. The analysis of the model (see Figure 6) suggests that the exosites of SK seem to potentially interact with some of the surface-exposed loops of substrate μPG, particularly those that are proximal to the activation peptide bond. SK exosites being at the rim of the active-site cleft seems to modulate the subsequent catalysis of the docked substrate. Close examination of the model predicts that the hydrophobic patch formed by the side chains of Ile88 and Val91 of the 88−97 loop of SK and residues Val624 and Leu626 of the calcium binding loop of substrate μPG appears to contribute toward the surface complementarities involved in substrate binding (Figure 7A). In addition, a cluster of positively and negatively charged

dx.doi.org/10.1021/bi400142s | *Biochemistry* 2013, 52, 8957−8968

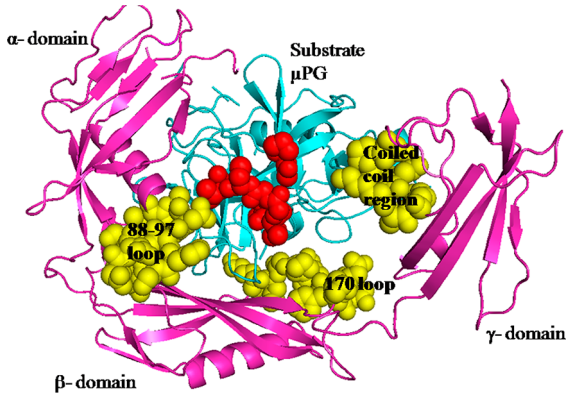

Figure 6. Putative ternary interaction model of partner and substrate μPG interaction(s) showing the disposition of various exosites. The ternary interaction model of the μPN·SK·μPN complex was generated by ZDOCK. The partner μPN of the SK·μPN complex is hidden for clarity. The three domains of SK are shown in magenta, with the exosites, namely, the 88−97 loop, 170 loop, and the coiled-coil region, shown in yellow. The activation loop (red) of the substrate μPG (cyan) is optimally positioned in the SK·μPN complex and is seen to be surrounded uniformly by the three exosites of SK.

residues in the 170 loop of SK appear to provide a strong electrostatic component for the optimal interaction with the substrate HPG. The importance of these interactions can be inferred, for example, from the catalytic contribution of Lys180 in the 170 loop during HPG activation as identified earlier through alanine mutagenesis.[12] One can see that the ε-amino group of Lys180 in the 170 loop is within 8−10 Å distance from the aromatic ring of Phe587 of the 37 loop, and that they seem to potentially interact through noncovalent ionic interactions (Figure 7B). Interestingly, the flexibility and surface accessibility of the side chains of other residues in the 170 loop, namely, Asp173, Asp174, and Arg176 also seem to potentially allow them to make ionic interactions with the residues of the 60 loop of substrate μPG (another surface-exposed loop), namely, Glu606, Lys607, and Arg610. The constellation of charged residues in the coiled-coil region of the γ domain of SK, especially, Asp322, Arg324, Asp328, Asp325, Arg330, Asp331, Lys332, and Lys334 participate in an extended network of salt-bridges and hydrogen bonds within the coiled-coil region as well as with the catalytic domain of the substrate. Residues Asp328 and Lys334 of the coiled-coil region seem to closely interact with residues of the methionine loop and the 186 loop of substrate μPG. A salt-bridge between Arg330 of SK and Glu714 of the methionine loop of substrate μPG is potentially positioned so as to provide a rigidifying anchor to facilitate optimal substrate interaction (see Figure 7C). Overall, these results indicate that these exosites confer specificity for interactions with the macromolecular substrate and that these interactions may play an important role in catalysis, steps subsequent to the binding of the substrate with the activator−enzyme complex.

DISCUSSION

One of the most interesting mechanistic insights that emerge from the present study is the discovery of co-operativity between the exosites of SK during substrate HPG processing by the SK·HPN activator complex, namely, the 88−97 and 170 loops, and the coiled-coil region. Although earlier studies[9,16,49] had succeeded in identifying these distinct substrate HPG-

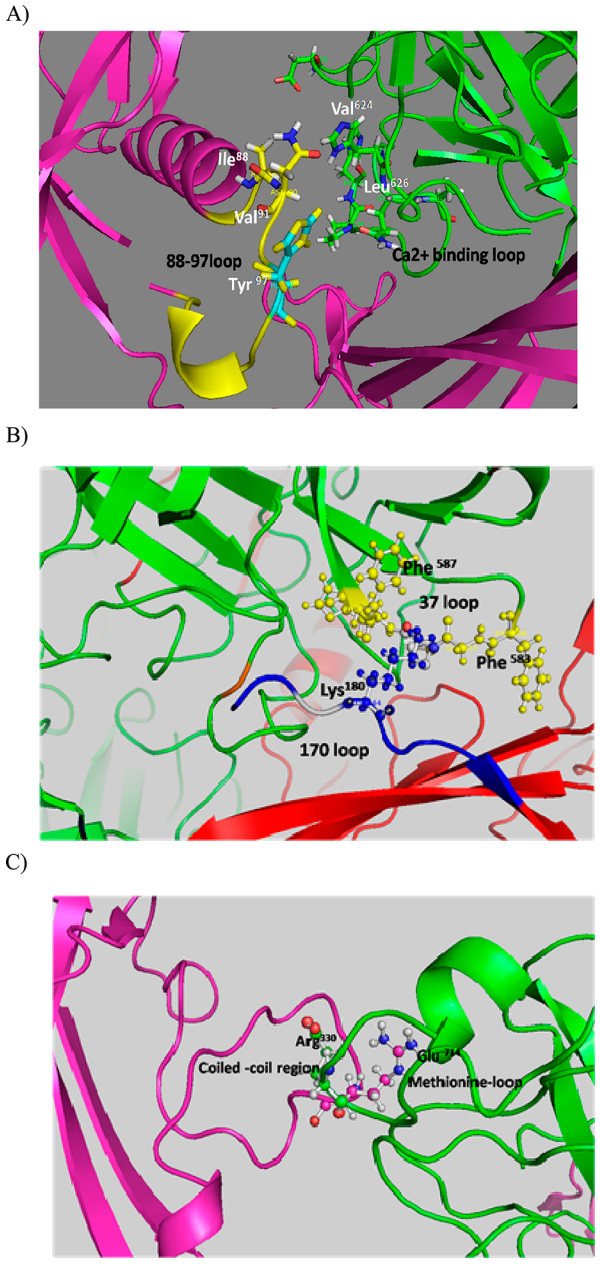

Figure 7. Putative model of substrate μPG interaction(s) with the SK exosites. (A) The inset shows a picture of the interactions between the SK 88−97 loop and the calcium binding loop of substrate μPG. (B) Snap shot of interactions between the SK 170 loop and the 37 loop of substrate μPG. (C) Close-up of interactions between the SK coiled-coil region and the methionine loop of substrate μPG. Molecular modeling was performed as described under Experimental Procedures.

specific exosites in the different domains of SK, the manner in which these operate during catalysis was unclear. Conventional thinking would suggest that a substrate-specific exosite would essentially be important for enzyme−substrate affinity; in contrast, the present results indicate that the SK exosites are important for processing of the substrate. The effects of mutations of these exosites in the whole protein largely manifest as k_{cat} effects, with relatively minor alterations in K_m for substrate HPG. In addition, the mutational studies clearly show a synergistic trend in the decline of catalytic rates for HPG activation as the exosite mutational load increases from a monosite to dual-site and to a three-site level in SK.

dx.doi.org/10.1021/bi400142s | *Biochemistry* 2013, 52, 8957−8968

Furthermore, molecular modeling studies suggest that there is the intriguing possibility that exosite-mediated interactions contribute toward the correct stereochemical placement of the scissile peptide bond in substrate HPG into the active center of the SK·HPN enzyme complex and thus participate in subsequent catalytic events, followed by the release of product HPN. Recently, crystal structures for full-length human plasminogen (HPG) (types I and II)[50] have been determined. These structures have the activation loop and cleavage site (Arg561−Val562) seemingly buried by the kringle domains and thus represent the closed conformation of HPG (see Figure S3, Supporting Information). Moreover, in these structures, the lysine binding site (LBS) in kringle 5 is occupied by Lys 50 of the plasminogen activation peptide (Pap) domain. Earlier studies have conclusively shown that in the SK·HPG ternary complex the LBS in kringle 5 interacts with the 250 loop in the β domain of SK.[18] Thus, at the very least, some changes in the orientation of the kringle domains would be a prerequisite for the plasminogen molecule to adopt a conformation conducive for catalysis by the SK·HPG complex. Interestingly, multiple conformations for kringle 5 have been observed in the two plasminogen molecules constituting the asymmetric unit (PDB ID: 4DUR).[50] These mobile conformations for kringle 5 evidently demonstrate that this domain can indeed have different orientations with respect to the catalytic domain, in various open or closed conformations.[50] Computational modeling of these conformational changes within full-length HPG would be a challenge and require additional experimental support. Therefore, it is unlikely that the presently available X-ray crystal structure for full-length HPG can be directly employed to model interactions between the SK·HPN binary complex and kringle domains of substrate plasminogen. Indeed, ongoing studies in our laboratory employing small-angle X-ray scattering suggest significant conformational changes in the substrate kringles upon docking into the activator complex (Singh, Kumar, Ashish, and Sahni, unpublished work).

The role of exosites in generating substrate specificity has been uncovered in various blood proteinases,[51] the prototypical example of exosite-regulated allosteric proteinase being thrombin.[52,53] Several lines of evidence suggest that, unlike the exosites of SK, the ones existent in coagulation proteases play a major role in augmenting substrate affinity and thus engendering the high specificity in these proteases, where substrate docking at the active site contributes to efficient catalysis.[54] Involvement of exosite-directed interactions in the catalytic mechanism leading to the inactivation of factor VIIIa by activated protein C (APC)[55,56] has also been reported. However, little information before the present study existed related to the global interactions of different exosites in SK during substrate HPG activation. In contrast to exosite systems such as the blood coagulation proteinases, the present study has revealed a high-order of synergy existing at the level of catalytic processing of substrate HPG, wherein substrate affinity per se for the macromolecular substrate remains essentially unaltered (an attribute that probably emanates from the burial of surfaces between the SK·HPN valley and HPG; see ref 4). However, besides the three catalytically important exosites examined in this work, the role of substrate kringles is also important. Deletion of these structures, particularly the fifth and fourth kringles, in the substrate decreases the catalytic rates by several fold.[14,57] One kringle-centric epitope that predominantly contributes toward substrate−enzyme affinity per se is the 250 loop, which is resident in the β domain of SK.[18,19] Thus, a combination of two distinct types of structural elements, the three exosites that are focused toward the serine protease domain of substrate with low affinity and the 250 loop, targeted toward the kringle domains with relatively higher affinity, appear to be important for catalysis. Together, these exosites co-operate to produce the high rates of HPG activation exhibited by the SK·HPN activator enzyme. Besides this important mechanistic insight, there are still several immediate questions that need to be addressed in future studies. As an example, one needs to identify the cognate sites in the substrate HPG which co-operate with the SK-contributed exosites. They may be important not only in stabilizing enzyme−substrate interactions but also in postdocking events, such as product expulsion and release. These mechanistic insights have also the potential to help design improved streptokinase-based thrombolytic drugs,[42,58] and indeed, some lead molecules based on earlier structure−function work are already under clinical development.[59] A more general fundamental insight into the mode of action of substrate-specificity-conferring exosites may also enable the engineering of altogether new substrate-specific proteolytic entities with useful functions.

■ ASSOCIATED CONTENT

Supporting Information

Mass spectra of the three peptides; inhibition of SK·HPN activator activity by three peptides; cartoon representation for domain organization of HPG; and a comparison of secondary structure of the peptides predicted through circular dichorism and X-ray diffraction data of the SK β domain, SK·HPN complex. This material is available free of charge via the Internet at http://pubs.acs.org.

■ AUTHOR INFORMATION

Corresponding Author

*Phone: 0172-2690830. Fax: +91-172-2690585. E-mail: sahni@imtech.res.in.

Funding

This study was largely supported by intramural funds from CSIR, India.

Notes

The authors declare no competing financial interest.

■ ACKNOWLEDGMENTS

We thank Paramjit Kaur, Deepak Bhatt, and Sharanjot Kaur for expert technical support and Dr. Subita Basu of the Blood Bank, Govt. Medical College, Chandigarh for human plasma.

■ ABBREVIATIONS

5-IAF, 5-(iodoacetamido) fluorescein; APC, activated protein C; ATA-FPR-CK, N^{α}[(acetylthio) acetyl]-D-Phe-Pro-Arg-CH_2Cl; μPG, microplasminogen; μPN, microplasmin; BSA, bovine serum albumin; CD, circular dichroism; DEAE, diethylaminoethyl-sepharose; DSSP, define secondary structure of proteins; DTNB, 5,5′-dithiobis-(2-nitrobenzoic acid); EACA, ϵ-aminocaproic acid; ESI, electron spray ionization; HIC, hydrophobic interaction chromatography; HPG, human plasminogen; HPN, human plasmin; IBs, inclusion bodies; IPTG, isopropyl-1-thio-β-D-galactopyranoside; k_{cat}, rate of catalysis at substrate saturation; K_D, equilibrium rate constant; K_m, Michaelis−Menton constant; k_{off}, rate of dissociation; k_{on}, rate of association; LBS, lysine binding site; MALDI, Matrix assisted laser desorption ionization; MetAP, methionine

aminopeptidase; NPGB, *p*-nitrophenyl *p*-guanidinobenzoate; PAP, plasminogen activation peptide; *wt*SK, wild type streptokinase; PAGE, polyacrylamide gel electrophoresis; RP-HPLC, reverse phase, high pressure liquid chromatography; SA, streptavidin; SAK, staphylokinase; SATA, succinimidyl (acetylthio)acetate; SDS, sodium dodecyl sulfate; SK, streptokinase; SPR, surface plasmon resonance; STI, soybean trypsin inhibitor; UK, urokinase; μPG, microplasminogen; μPN, microplasmin

REFERENCES

(1) McClintock, D. K., and Bell, P. H. (1971) The mechanism of activation of human plasminogen by streptokinase. *Biochem. Biophys. Res. Commun. 43*, 694−702.

(2) Bajaj, A. P., and Castellino, F. J. (1977) Activation of human plasminogen by equimolar levels of streptokinase. *J. Biol. Chem. 252*, 492−498.

(3) Boxrud, P. D., Verhamme, I. M., and Bock, P. E. (2004) Resolution of conformational activation in the kinetic mechanism of plasminogen activation by streptokinase. *J. Biol. Chem. 279*, 36633−36641.

(4) Wang, X., Lin, X., Loy, J. A., Tang, J., and Zhang, X. C. (1998) Crystal structure of the catalytic domain of human plasmin complexed with streptokinase. *Science 281*, 1662−1665.

(5) Boxrud, P. D., and Bock, P. E. (2004) Coupling of conformational and proteolytic activation in the kinetic mechanism of plasminogen activation by streptokinase. *J. Biol. Chem. 279*, 36642−36649.

(6) Boxrud, P. D., Fay, W. P., and Bock, P. E. (2000) Streptokinase binds to human plasmin with high affinity, perturbs the plasmin active site, and induces expression of a substrate recognition exosite for plasminogen. *J. Biol. Chem. 275*, 14579−14589.

(7) Markus, G., and Werkheiser, W. C. (1964) The Interaction of streptokinase with plasminogen. I. Functional properties of the activated enzyme. *J. Biol. Chem. 239*, 2637−2643.

(8) Parrado, J., Conejero-Lara, F., Smith, R. A., Marshall, J. M., Ponting, C. P., and Dobson, C. M. (1996) The domain organization of streptokinase: nuclear magnetic resonance, circular dichroism, and functional characterization of proteolytic fragments. *Protein Sci. 5*, 693−704.

(9) Nihalani, D., Raghava, G. P., and Sahni, G. (1997) Mapping of the plasminogen binding site of streptokinase with short synthetic peptides. *Protein Sci. 6*, 1284−1292.

(10) Boxrud, P. D., and Bock, P. E. (2000) Streptokinase binds preferentially to the extended conformation of plasminogen through lysine binding site and catalytic domain interactions. *Biochemistry 39*, 13974−13981.

(11) Yadav, S., Datt, M., Singh, B., and Sahni, G. (2008) Role of the 88−97 loop in plasminogen activation by streptokinase probed through site-specific mutagenesis. *Biochim. Biophys. Acta 1784*, 1310−1318.

(12) Aneja, R., Datt, M., Singh, B., Kumar, S., and Sahni, G. (2009) Identification of a new exosite involved in catalytic turnover by the streptokinase-plasmin activator complex during human plasminogen activation. *J. Biol. Chem. 284*, 32642−32650.

(13) Lee, P. P., Wohl, R. C., Boreisha, I. G., and Robbins, K. C. (1988) Kinetic analysis of covalent hybrid plasminogen activators: effect of CNBr-degraded fibrinogen on kinetic parameters of Glu1-plasminogen activation. *Biochemistry 27*, 7506−7513.

(14) Sundram, V., Nanda, J. S., Rajagopal, K., Dhar, J., Chaudhary, A., and Sahni, G. (2003) Domain truncation studies reveal that the streptokinase-plasmin activator complex utilizes long range protein-protein interactions with macromolecular substrate to maximize catalytic turnover. *J. Biol. Chem. 278*, 30569−30577.

(15) Loy, J. A., Lin, X., Schenone, M., Castellino, F. J., Zhang, X. C., and Tang, J. (2001) Domain interactions between streptokinase and human plasminogen. *Biochemistry 40*, 14686−14695.

(16) Nihalani, D., Kumar, R., Rajagopal, K., and Sahni, G. (1998) Role of the amino-terminal region of streptokinase in the generation of a fully functional plasminogen activator complex probed with synthetic peptides. *Protein Sci. 7*, 637−648.

(17) Wang, X., Tang, J., Hunter, B., and Zhang, X. C. (1999) Crystal structure of streptokinase beta-domain. *FEBS Lett. 459*, 85−89.

(18) Dhar, J., Pande, A. H., Sundram, V., Nanda, J. S., Mande, S. C., and Sahni, G. (2002) Involvement of a nine-residue loop of streptokinase in the generation of macromolecular substrate specificity by the activator complex through interaction with substrate kringle domains. *J. Biol. Chem. 277*, 13257−13267.

(19) Tharp, A. C., Laha, M., Panizzi, P., Thompson, M. W., Fuentes-Prior, P., and Bock, P. E. (2009) Plasminogen substrate recognition by the streptokinase-plasminogen catalytic complex is facilitated by Arg253, Lys256, and Lys257 in the streptokinase beta-domain and kringle 5 of the substrate. *J. Biol. Chem. 284*, 19511−19521.

(20) Wu, D. H., Shi, G. Y., Chuang, W. J., Hsu, J. M., Young, K. C., Chang, C. W., and Wu, H. L. (2001) Coiled coil region of streptokinase gamma-domain is essential for plasminogen activation. *J. Biol. Chem. 276*, 15025−15033.

(21) Yadav, S., Aneja, R., Kumar, P., Datt, M., Sinha, S., and Sahni, G. (2011) Identification through combinatorial random and rational mutagenesis of a substrate-interacting exosite in the gamma domain of streptokinase. *J. Biol. Chem. 286*, 6458−6469.

(22) Deutsch, D. G., and Mertz, E. T. (1970) Plasminogen: purification from human plasma by affinity chromatography. *Science 170*, 1095−1096.

(23) Chaudhary, A., Vasudha, S., Rajagopal, K., Komath, S. S., Garg, N., Yadav, M., Mande, S. C., and Sahni, G. (1999) Function of the central domain of streptokinase in substrate plasminogen docking and processing revealed by site-directed mutagenesis. *Protein Sci. 8*, 2791−2805.

(24) Bock, P. E. (1992) Active-site-selective labeling of blood coagulation proteinases with fluorescence probes by the use of thioester peptide chloromethyl ketones. II. Properties of thrombin derivatives as reporters of prothrombin fragment 2 binding and specificity of the labeling approach for other proteinases. *J. Biol. Chem. 267*, 14974−14981.

(25) Bock, P. E. (1993) Thioester peptide chloromethyl ketones: reagents for active site-selective labeling of serine proteinases with spectroscopic probes. *Methods Enzymol. 222*, 478−503.

(26) Radek, J. T., Davidson, D. J., and Castellino, F. J. (1993) Streptokinase-plasmin(ogen) activator assays. *Methods Enzymol. 223*, 145−155.

(27) Wohl, R. C., Summaria, L., and Robbins, K. C. (1980) Kinetics of activation of human plasminogen by different activator species at pH 7.4 and 37 degrees C. *J. Biol. Chem. 255*, 2005−2013.

(28) Shi, G. Y., Chang, B. I., Chen, S. M., Wu, D. H., and Wu, H. L. (1994) Function of streptokinase fragments in plasminogen activation. *Biochem. J. 304* (Pt 1), 235−241.

(29) Wakeham, N., Terzyan, S., Zhai, P., Loy, J. A., Tang, J., and Zhang, X. C. (2002) Effects of deletion of streptokinase residues 48−59 on plasminogen activation. *Protein Eng. 15*, 753−761.

(30) Chase, T., Jr., and Shaw, E. (1969) Comparison of the esterase activities of trypsin, plasmin, and thrombin on guanidinobenzoate esters. Titration of the enzymes. *Biochemistry 8*, 2212−2224.

(31) Wohl, R. C. (1984) Interference of active site specific reagents in plasminogen-streptokinase active site formation. *Biochemistry 23*, 3799−3804.

(32) Parry, M. A., Fernandez-Catalan, C., Bergner, A., Huber, R., Hopfner, K. P., Schlott, B., Guhrs, K. H., and Bode, W. (1998) The ternary microplasmin-staphylokinase-microplasmin complex is a proteinase-cofactor-substrate complex in action. *Nat. Struct. Biol. 5*, 917−923.

(33) Chen, R., Li, L., and Weng, Z. (2003) ZDOCK: an initial-stage protein-docking algorithm. *Proteins 52*, 80−87.

(34) Dawson, K. M., Marshall, J. M., Raper, R. H., Gilbert, R. J., and Ponting, C. P. (1994) Substitution of arginine 719 for glutamic acid in

human plasminogen substantially reduces its affinity for streptokinase. *Biochemistry 33*, 12042−12047.
(35) Jespers, L., Van Herzeele, N., Lijnen, H. R., Van Hoef, B., De Maeyer, M., Collen, D., and Lasters, I. (1998) Arginine 719 in human plasminogen mediates formation of the staphylokinase:plasmin activator complex. *Biochemistry 37*, 6380−6386.
(36) Jackson, K. W., and Tang, J. (1982) Complete amino acid sequence of streptokinase and its homology with serine proteases. *Biochemistry 21*, 6620−6625.
(37) Kabsch, W., and Sander, C. (1983) Dictionary of protein secondary structure: pattern recognition of hydrogen-bonded and geometrical features. *Biopolymers 22*, 2577−2637.
(38) Joosten, R. P., te Beek, T. A., Krieger, E., Hekkelman, M. L., Hooft, R. W., Schneider, R., Sander, C., and Vriend, G. (2011) A series of PDB related databases for everyday needs. *Nucleic Acids Res. 39*, D411−D419.
(39) Lin, L. F., Oeun, S., Houng, A., and Reed, G. L. (1996) Mutation of lysines in a plasminogen binding region of streptokinase identifies residues important for generating a functional activator complex. *Biochemistry 35*, 16879−16885.
(40) Radek, J. T., and Castellino, F. J. (1989) Conformational properties of streptokinase. *J. Biol. Chem. 264*, 9915−9922.
(41) De Renzo, E. C., Siiteri, P. K., Hutchings, B. L., and Bell, P. H. (1967) Preparation and certain properties of highly purified streptokinase. *J. Biol. Chem. 242*, 533−542.
(42) Reed, G. L., Houng, A. K., Liu, L., Parhami-Seren, B., Matsueda, L. H., Wang, S., and Hedstrom, L. (1999) A catalytic switch and the conversion of streptokinase to a fibrin-targeted plasminogen activator. *Proc. Natl. Acad. Sci. U.S.A. 96*, 8879−8883.
(43) Wang, S., Reed, G. L., and Hedstrom, L. (2000) Zymogen activation in the streptokinase-plasminogen complex. Ile1 is required for the formation of a functional active site. *Eur. J. Biochem. 267*, 3994−4001.
(44) Boxrud, P. D., Verhamme, I. M., Fay, W. P., and Bock, P. E. (2001) Streptokinase triggers conformational activation of plasminogen through specific interactions of the amino-terminal sequence and stabilizes the active zymogen conformation. *J. Biol. Chem. 276*, 26084−26089.
(45) Gonzalez-Gronow, M., Siefring, G. E., Jr., and Castellino, F. J. (1978) Mechanism of activation of human plasminogen by the activator complex, streptokinase-plasmin. *J. Biol. Chem. 253*, 1090−1094.
(46) Bock, P. E., Day, D. E., Verhamme, I. M., Bernardo, M. M., Olson, S. T., and Shore, J. D. (1996) Analogs of human plasminogen that are labeled with fluorescence probes at the catalytic site of the zymogen. Preparation, characterization, and interaction with streptokinase. *J. Biol. Chem. 271*, 1072−1080.
(47) Robbins, K. C., Wohl, R. C., and Summaria, L. (1981) Plasmin and plasminogen activators: kinetics, and kinetics of plasminogen activation. *Ann. N.Y. Acad. Sci. 370*, 588−591.
(48) Summaria, L., Wohl, R. C., Boreisha, I. G., and Robbins, K. C. (1982) A virgin enzyme derived from human plasminogen. Specific cleavage of the arginyl-560-valyl peptide bond in the diisopropoxyphosphinyl virgin enzyme by plasminogen activators. *Biochemistry 21*, 2056−2059.
(49) Nihalani, D., and Sahni, G. (1995) Streptokinase contains two independent plasminogen-binding sites. *Biochem. Biophys. Res. Commun. 217*, 1245−1254.
(50) Law, R. H., Caradoc-Davies, T., Cowieson, N., Horvath, A. J., Quek, A. J., Encarnacao, J. A., Steer, D., Cowan, A., Zhang, Q., Lu, B. G., Pike, R. N., Smith, A. I., Coughlin, P. B., and Whisstock, J. C. (2012) The X-ray crystal structure of full-length human plasminogen. *Cell Rep. 1*, 185−190.
(51) Bock, P. E., Panizzi, P., and Verhamme, I. M. (2007) Exosites in the substrate specificity of blood coagulation reactions. *J. Thromb. Haemostasis 5* (Suppl 1), 81−94.
(52) Boskovic, D. S., Troxler, T., and Krishnaswamy, S. (2004) Active site-independent recognition of substrates and product by bovine prothrombinase: a fluorescence resonance energy transfer study. *J. Biol. Chem. 279*, 20786−20793.
(53) Orcutt, S. J., Pietropaolo, C., and Krishnaswamy, S. (2002) Extended interactions with prothrombinase enforce affinity and specificity for its macromolecular substrate. *J. Biol. Chem. 277*, 46191−46196.
(54) Krishnaswamy, S. (2005) Exosite-driven substrate specificity and function in coagulation. *J. Thromb. Haemostasis 3*, 54−67.
(55) Varfaj, F., Wakabayashi, H., and Fay, P. J. (2007) Residues surrounding Arg336 and Arg562 contribute to the disparate rates of proteolysis of factor VIIIa catalyzed by activated protein C. *J. Biol. Chem. 282*, 20264−20272.
(56) Manithody, C., Fay, P. J., and Rezaie, A. R. (2003) Exosite-dependent regulation of factor VIIIa by activated protein C. *Blood 101*, 4802−4807.
(57) Joshi, K. K., Nanda, J. S., Kumar, P., and Sahni, G. (2012) Substrate kringle-mediated catalysis by the streptokinase-plasmin activator complex: critical contribution of kringle-4 revealed by the mutagenesis approaches. *Biochim. Biophys. Acta 1824*, 326−333.
(58) Marder, V. J. (1993) Recombinant streptokinase: opportunity for an improved agent. *Blood Coagulation Fibrinolysis 4*, 1039−1040.
(59) Jayaraman, K. (2012) Novel Indian clotbuster. *Nat. Biotechnol. 30*, 904.